JOURNAL OF MATERIALS SCIENCE **37** (2002) 2011–2016

Effects of BaO on the glass formation of the PbO-B_2O_3-TiO_2-BaO system in relation to transition temperatures

SEON WOO LEE, KWANG BO SHIM, KEUN HO AUH
Department of Ceramic Engineering, CPRC, Hanyang University, Seoul 133-791, Korea
E-mail: kbshim@hanyang.ac.kr

The variation of the BaO content on the quaternary PbO-B_2O_3-TiO_2-BaO system's glass formation tendency was investigated in relation to transition temperatures, such as melt temperature (T_f), liquidus temperature (T_l), crystallization temperature (T_c) and glass transition temperature (T_g). Compositions were melted between 800°C and 1300°C. In order to obtain bulk glass samples, glass formation was carried out using a preheated cylindrical brass mould without forcing the cooling rate to increase. Glass formation tendency increased with increasing the temperature ratios of T_g/T_l and T_c/T_l and with decreasing T_g/T_c. Eutectic compositions preferentially formed glasses from melts due to their low melting temperatures. © *2002 Kluwer Academic Publishers*

1. Introduction

Glass-ceramics [1–3] have been widely used in the electrical/electronic industry using some unique advantages of glass processing such as versatility of fabrication and specific features such as pore-free, low crystallization temperature and narrow-distribution fine grains by controlled crystallization. However, ferroelectric glass-ceramics have not drawn much attention and only a few reports about lead titanate glass or glass-ceramic processes have been made [4–10]. $PbTiO_3$ glass samples in these reports were produced mainly by a rapid twin roller quenching technique [11].

To produce a stable $PbTiO_3$ glass, it is necessary to add a glass former such as SiO_2 or B_2O_3 and/or modifiers such as alkaline or alkali rare-earth species. This fact suggests that it is difficult to produce $PbTiO_3$ glasses containing a high volume fraction of $PbTiO_3$ using the conventional cooling method in which a glass is fabricated by natural cooling of a melt. Furthermore, it is rare to detail the microstructures and ferroelectric properties of the $PbTiO_3$ glass-ceramic samples. This may reflect the poor properties of the glass-ceramics compared to those of the ceramics derived from powder sintering or sol-gel processes, which arise from the small volume fraction of $PbTiO_3$ crystals and the high volume fraction of glassy phases. For the production of stable glasses where a high volume fraction of a crystalline phases can by precipitated by a controlled heat treatment, it is of importance to investigate some factors deciding the glass formation of a glass-forming system.

A glass formation tendency of a glass-forming system is governed by nucleation and crystal growth that take place during cooling from the melt [12]. This phase transformation is directly related to a transition temperature such as the liquidus temperature, crystallization temperature and glass transition temperature, which purely depend on glass compositions. These factors can be controlled by manipulating the glass composition, thereby being critical in the design of the starting composition to fabricate a stable glass. In general, a quaternary system offers more flexibility in the glass formation than a binary system or a ternary system. The present authors adopted the quaternary glass system of 30PbO-$(40 - x)B_2O_3$-30$TiO_2 - x$BaO (mol%) to investigate the glass formation tendency by correlating the transition temperatures of the as-solidified glasses with varying BaO content.

2. Experimental procedures

Starting compositions were prepared by weighing reagent-grade oxide powders, mixing them in a porcelain mortar with a small amount of acetone, then drying in an oven at 120°C (compositions in Table I). The dried mixture was heated at 400°C for 30 min to remove water and acetone, so that an abrupt volatile reaction could be avoided during melting. Melting was carried out in a Pt crucible between 800°C and 1300°C for 10 min–20 min. the melt of 20 gr-40 gr per batch was cast in a brass mould preheated at 400°C, whose dimensions were 40 mm in height and 10 mm in diameter. The weight of the starting composition was chosen to have approximately a constant melt volume fitting into the casting volume of the mould. In order to confirm whether the melt of a given composition forms a glass by natural cooling, the melting-casting procedure was repeated 3 or 4 times by changing the melting temperature (designated as the glass formation temperature, GFT, hereinafter to avoid a confusion with the thermodynamic melting temperature) up to 1300°C.

0022–2461

TABLE I Lead titanate glass composition and solidification results

Sample no.	Initial composition (mol%)				GFT[a] T_f °C	Glass formation	Transition temperature °C (measured by DTA)			
	PbO	B_2O_3	TiO_2	BaO			T_g	T_c[b]	T_l	T_l[c]
PBT1	55	30	15	0	1100	CR	–	–	–	–
PBT3	60	30	10	0	1080	GL	469	552	706	601
PBT4	30	40	30	0	1300	CR	–	–	–	–
PBT5	40	30	30	0	1260	PC	–	–	–	–
PBTB2-2	30	37.5	30	2.5	1170	CR	–	–	–	–
PBTB2-3	30	35	30	5	1260	PC	484	557	847	893
PBTB2-4	30	32.5	30	7.5	1160	GL	481	584	900	910
PBTB2-5	30	30	30	10	1120	GL	471	598	727	893
PBTB2-6	30	27.5	30	12.5	1040	GL	450	600	761	885
PBTB2-7	30	25	30	15	1100	GL	455	587	775	905
PBTB2-8	30	22.5	30	17.5	1130	GL	456	570	791	926
PBTB2-9	30	20	30	20	1220	GL	440	543	866	964
PBTB2-10	30	15	30	25	1300	CR	–	–	–	–

[a] Glass formation temperature: the temperature at which the starting composition is melted.

[b] The first exothermic peak for $PbTiO_3$ crystallization in Fig. 6.

[c] Measured using a hot-stage microscope.

Microstructures of the as-solidified samples were investigated using SEM (scanning electron microscopy) and TEM (transmission electron microscopy). Chemical analyses were carried out by EDXA (energy dispersive X-ray analysis) and XRF (X-ray fluorescence). Transition temperatures were measured using DTA (differential thermal analysis) and a hot-stage microscope.

3. Results and discussion

Solidification of the melt was carried out for glass formation throughout a systematic investigation for ternary and quaternary systems. The solidification results are listed in Table I with the initial compositions. The ternary lead titanate compositions (PbO-B_2O_3-TiO_2) were investigated as the preliminary experiments. In most ternary compositions, the melts did not solidify as glasses except for a few compositions, such as PBT3 ($60PbO$-$30B_2O_3$-$10TiO_2$ mol%), which contained relatively large proportions of lead and boric oxides but a small proportion of titanium oxide. When barium oxide was added to the ternary system as a modifier, the glass formation tendency was remarkably improved. The maximum amount of $PbOTiO_2$ (about 1 : 1 mole ratio) in the starting quaternary composition was 79 mol%.

In the quaternary glass system, the GFT ranged between 860°C and 1270°C depending on the composition. The as-solidified were classified into transparent glasses (GL), partly opaque/transparent crystallized samples (PC), and totally opaque crystallized samples (CR). The glasses obtained were transparent and yellowish. These transparent samples were clearly confirmed to be amorphous as shown by the typical bright field (BF) TEM image and the electron diffraction pattern in Fig. 1 and by X-ray diffraction patterns in Fig. 2a. In PC and CR samples, scattered opaque particles or wave/stripe forms were developed during cooling.

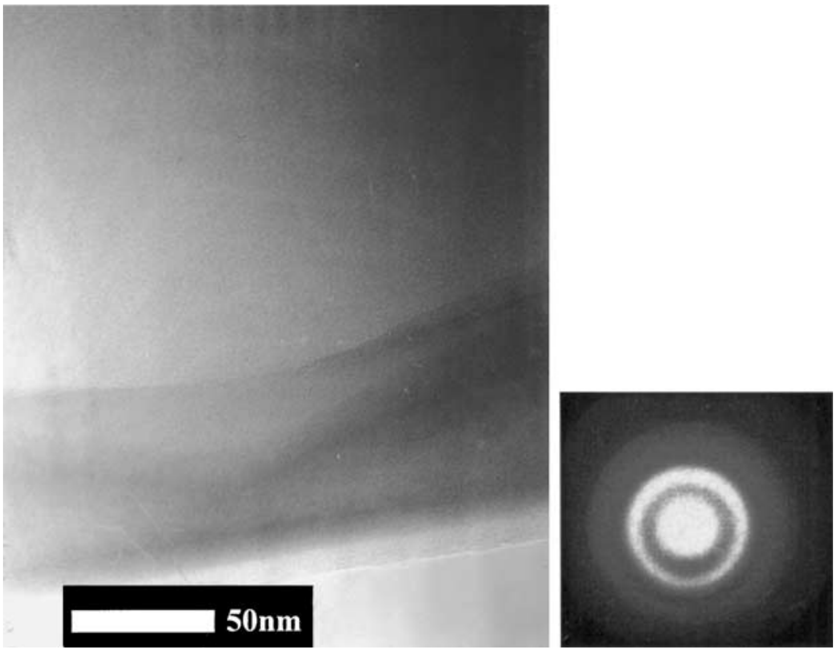

Figure 1 BF TEM image and selected area electron diffraction pattern of as-solidified glass whose composition is $30PbO$-$27.5B_2O_3$-$30TiO_2$-$12.5BaO$ (mol%).

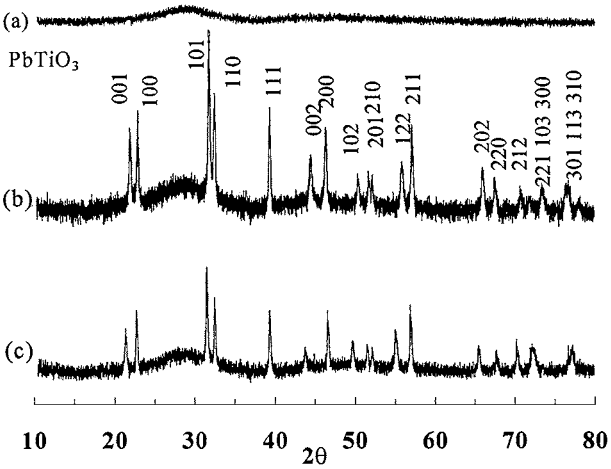

Figure 2 X-ray diffraction patterns for the as-solidified samples: (a) glass, (b) partly crystallized sample of 30PbO-22.5B_2O_3-30TiO_2-17.5BaO (mol%) and (c) partly crystallized sample of 60PbO-30B_2O_3-10TiO_2 (mol%).

The types of crystalline phases which occurred during cooling were determined by the BaO content in the composition and can be classified into two types. The first category is a very large acicular form of tetragonal TiO_2 or Ti-rich phases which were developed in the quaternary containing less than 7.5 mol% BaO. A typical example is shown in Fig. 3 together with its EDXA spectra. The occurrence of these Ti phases may indicate that phase separation took place in the melt or that TiO_2 particles were not completely dissolved in the melt. As shown by SEM images in Fig. 4 and XRD patterns in Fig. 2b and c, the second category is tetragonal $PbTiO_3$ crystals, which were formed in the quaternary composition containing more than 17.5 mol% BaO and in the ternary composition. Therefore, different types of crystalline phases and microstructure are expected when these transparent glasses with different compositions are crystallized.

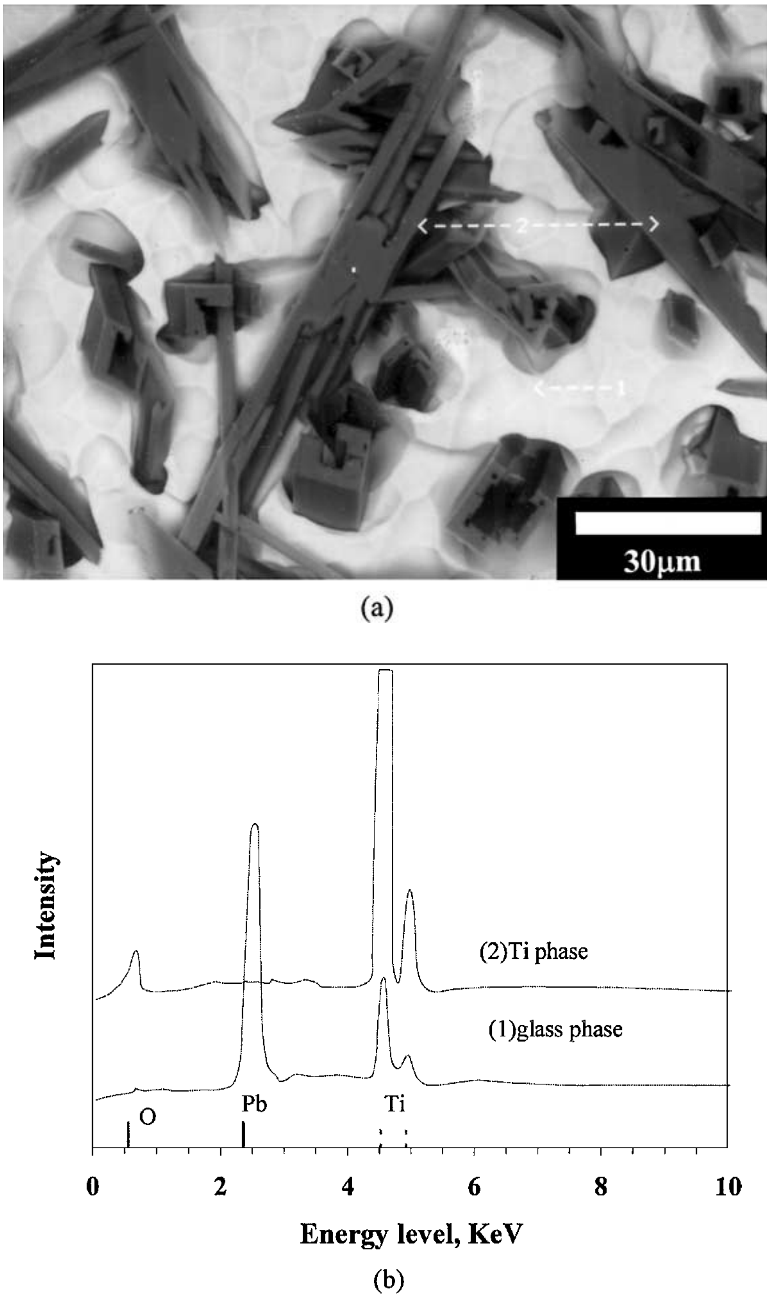

(a)

(b)

Figure 3 (a) Backscattered SEM image of a fracture surface and (b) EDXA spectra of an as-solidified sample of 30PbO-32.5B_2O_3-30TiO_2-7.5BaO (mol%).

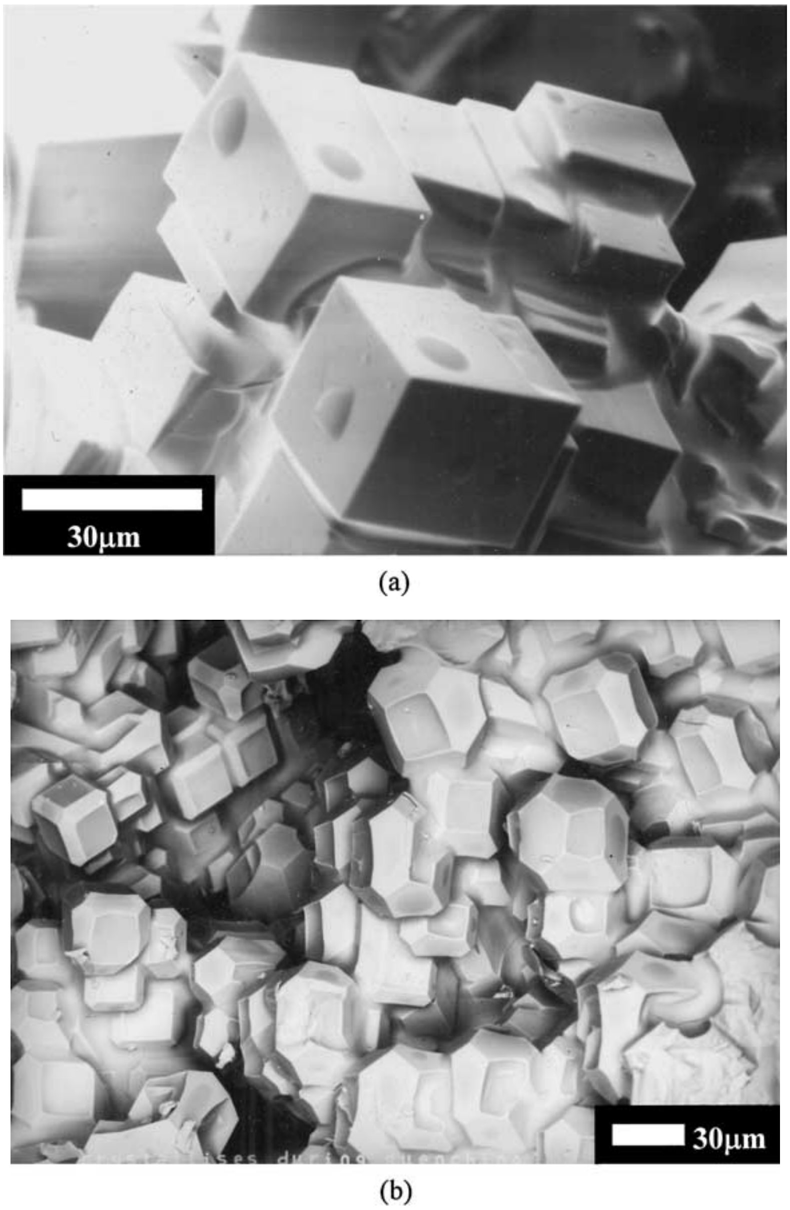

Figure 4 Backscattered SEM images of $PbTiO_3$ crystals formed during solidification of melts with the compositions of (a) $60PbO\text{-}30B_2O_3\text{-}10TiO_2$ and (b) $30PbO\text{-}22.5B_2O_3\text{-}30TiO_2\text{-}17.5BaO$ (mol%).

Quantitative analyses for the as-solidified glasses were carried out using XRF. The XRF results for Pb, Ti, and Ba elements are presented in Table II in weight fractions. Boron was not considered in this table because the boron atom is too light to be detected in the XRF equipment used. Table II shows that considerable losses of Pb and Ba were caused by interactive melting at high temperatures, so that the fraction of the Ti element had a corresponding increase. This increase in the fraction of Ti may cause the formation of Ti-rich pyrochlore phases during crystallization. Therefore, an excess amount of Pb must be added in the starting composition to compensate for this loss of Pb. It is also assumed that a considerable amount of B is volatilized due to the low melting temperature of B_2O_3.

To investigate the glass formation tendency in PBTB2 series compositions, the GFT was plotted as a function of the BaO content in Fig. 5. This figure shows 3 regions of glass formation, partly crystallized and crystallized zones. The glass formation tendency

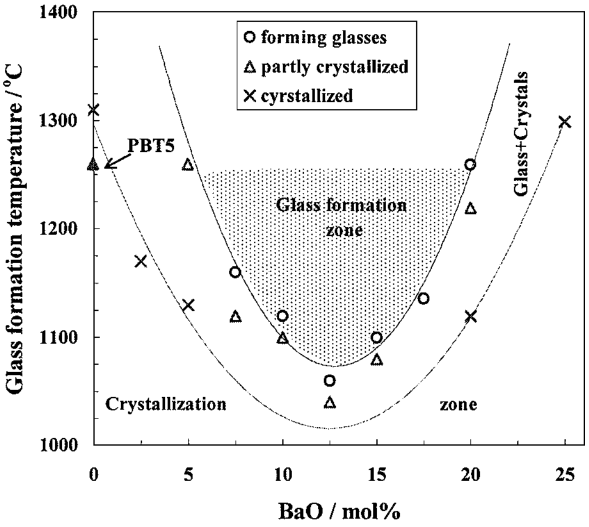

Figure 5 The glass formation ability with BaO content and glass formation (melting) temperature in the composition of $30PbO\text{-}(40\text{-}x)B_2O_3\text{-}30TiO_2\text{-}x BaO$ (mol%).

TABLE II XRF quantitative analysis

Sample no.	Composition, wt% PbO	TiO_2	BaO
	Starting composition before melting		
PBTB2-5	63.01	22.56	14.43
PBTB2-6	60.82	21.77	17.41
PBTB2-9	55.07	19.71	25.22
PBTB5-2	61.72	18.41	19.87
PBTB5-5	69.23	16.30	14.47
PBTB7-8	66.46	23.11	10.43
	Glass composition after solidification		
PBTB2-5	58.76 ± 0.77	28.26 ± 0.06	12.98 ± 0.63
PBTB2-6	62.22 ± 1.13	26.09 ± 0.06	11.68 ± 0.60
PBTB2-9	52.78 ± 0.16	28.86 ± 0.06	18.36 ± 0.74
PBTB5-2	56.07 ± 0.25	26.61 ± 0.06	17.32 ± 0.73
PBTB5-5	66.30 ± 1.33	21.63 ± 0.05	12.07 ± 0.62
PBTB7-8	56.94 ± 0.54	28.56 ± 0.06	14.50 ± 0.66

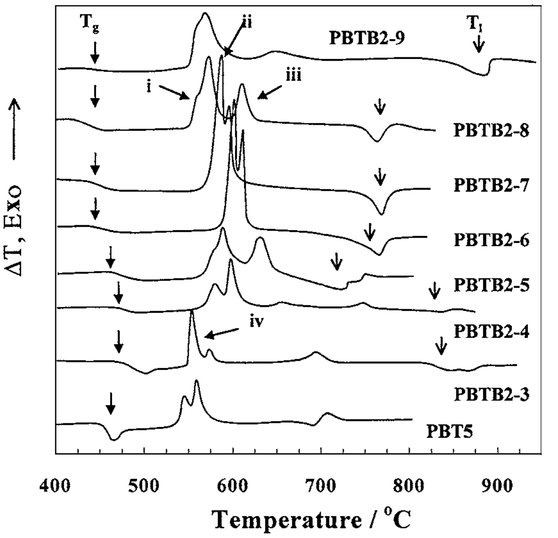

Figure 6 DTA curves of $PbTiO_3$ glasses (heating rate: 10°C min^{-1}, compositions in Table I.

was greatly influenced by the GFT and the BaO content. The GFT was a minimum of 1040°C at 12.5 mol% BaO and rapidly increased with the variation of the BaO content on both sides of this value, showing the eutectic effect [13]. Therefore, it can be concluded that the glass formation tendency is maximized at 12.5 mol% BaO and decreases as the BaO content deviates from the value of 12.5 mol%. Transparent glasses were obtained in the range between 7.5 mol% and 20 mol% BaO. Beyond this range, glasses were not formed by naturally cooling the melts. Fig. 5 also shows that for the same composition a higher GFT is preferred to produce the glass. This phenomenon could be related to phase separation or a change in the structure of the melt at a critical melting temperature.

Fig. 6 represents DTA curves of as-solidified glasses of PBTB2 series compositions, showing glass transition temperature T_g, crystallization temperature T_c. and liquidus temperature T_l, whose values are listed in Table I. The DTA curves show several exothermic peaks where $PbTiO_3$ metastable phases (i), $PbTiO_3$ crystals (ii), unknown barium-titanium-borate phases (iii) or Ti rich phases (iv) are formed depending on the glass composition. The glass transition temperature (marked as filled-arrows) and liquidus temperature (marked as line-arrows) have minimum values at about 10–12.5 mol% BaO, while the crystallization temperature has a maximum of 600°C at 12.5 mol% BaO (PBTB2-6). Compared to the glass formation tendency shown in Fig. 5, the change in these transition temperatures with the BaO content leads to the conclusion that the glass formation tendency increases with increasing T_c and decreasing T_g or T_l.

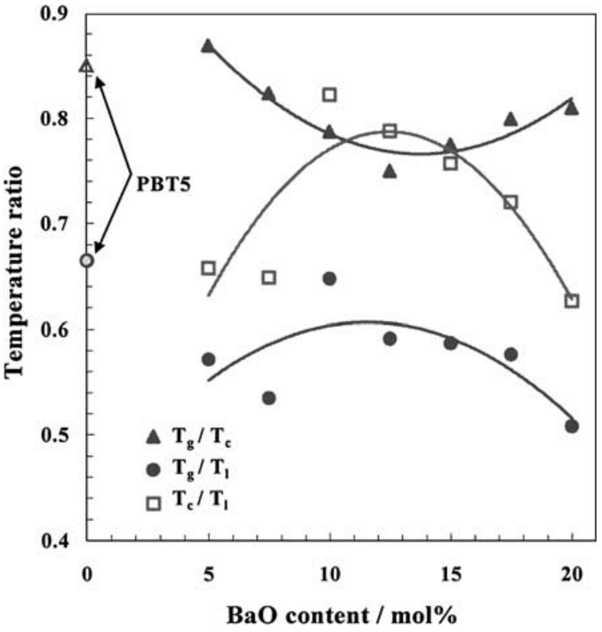

Figure 7 Temperature ratios between transition temperatures with variation of BaO content in the composition of 30PbO-(40-x)B_2O_3-30TiO_2-xBaO(mol%).

To investigate a correlation among T_g, T_c, and T_l, the temperature ratios of T_c/T_l, T_g/T_l and T_g/T_c were plotted as a function of the BaO content. Fig. 7 shows that the glass-forming ability increases with an increase of T_c/T_l or T_g/T_l and with a decrease of T_g/T_c. In other words, glass formation becomes easier as the temperature differences of T_l-T_g or T_l-T_c, are smaller and T_c-T_g is larger. These results indicate that a smaller value of T_l-T_g or T_l-T_c increase the possibility for the melt to bypass the crystallization zone, thus instantly to reach an appropriate viscosity where atomic rearrangements are difficult. When T_c-T_g values are smaller, on the other hand, crystallization will be likely to occur due to a small activation energy of nucleation and crystal growth.

The relation between the glass formation tendency and the transition temperature could be explained by introducing the viscosity of the melt. The viscosity of most glass-forming systems follows an empirical equation, known as the Vogel-Fulcher equation at a certain temperature range [14, 15].

$$\ln \eta = \frac{A}{T_r - T_{rg}} + B \tag{1}$$

Here A and B are constants, η is the viscosity, T_r the reduced temperature ($=T/T_f$) and $T_{rg} = T_g/T_f$. In this equation, the logarithmic viscosity of the melt is proportional to the reciprocal of T_r-T_{rg}. Under the

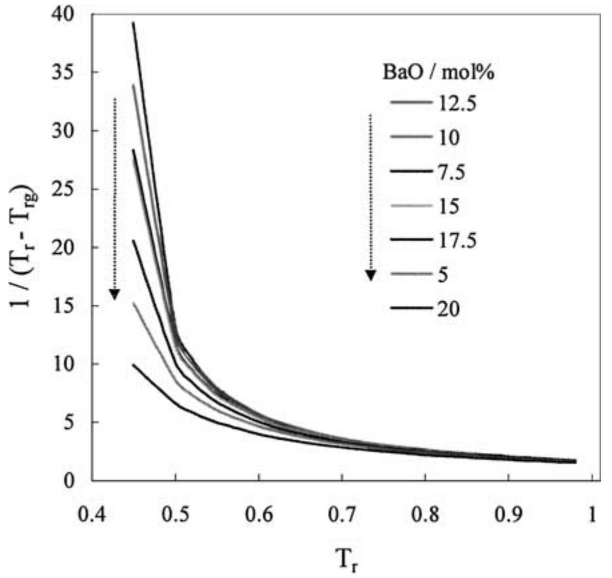

Figure 8 The reciprocal of $T_r - T_{rg}$ as a function of $T_r(T_r = T/T_f T_{rg} = T_g/T_f)$.

assumption that the glass system used in this study follows the Vogel-Fulcher relation, the plot of $1/(T_r\text{-}T_{rg})$ versus T_r is plotted in Fig. 8 with variation in the BaO content. This plot shows the glass-forming ability of a glass-forming liquid at a certain temperature during cooling from its melt.

Fig. 8 shows that the value of $1/(T_r\text{-}T_{rg})$ as a function of T_r is always largest at 12.5 mol% BaO (PBTB2-6), indicating that the temperature interval of cooling required for the glass formation is minimal. In addition, $1/(T_r\text{-}T_{rg})$ rapidly changes at about $T_r = 0.5$ and the increasing rate is also greatest at 12.5 mol% BaO. It is therefore assumed that an abrupt change in viscosity begins at this point and thus the temperature interval of cooling should be larger than $T_f/2$. The minimum interval of cooling for bypassing the crystallization zone can be estimated by introducing T_c/T_f. A larger value of T_c/T_f will decrease the probability of crystallization during cooling due to a smaller cooling interval and thus a relatively larger cooling rate at the initial cooling stage. Table III shows that the value of T_c/T_f is largest at 12.5 mol% BaO, while decreasing on the both sides of 12.5 mol% BaO. This tendency corresponds to the glass-forming tendency shown in Fig. 5. Since the rapid change in the viscosity begins at about $T_r = 0.5$, the glass-forming ability increases due to the easier bypass of the crystallization zone as T_c/T_f is bigger than about 0.5. If T_c/T_f is near or below 0.5, on the other hand, the probability of crystallization will increase and the glass formation will fail as long as the viscosity or the cooling rate is insufficient to suppress crystallization.

As a result, the transition temperature has a great influence on the glass-forming ability of a glass system and they are sensitively correlated with each other. There are many factors that should be considered to establish the criteria of glass-forming ability. Under the glass-forming conditions used in this study, the ratio or difference between the transition temperatures of glasses could be a useful criterion to estimate the glass formation ability of a glass system and thus to design an optimal glass system.

TABLE III The temperature interval of cooling required for by-passing crystallization

BaO (mol%)	0	5	7.5	10	12.5	15	17.5	20
T_c/T_f	0.438	0.442	0.503	0.534	0.566	0.534	0.502	0.431

4. Conclusions

Glass formation tendency was markedly improved when BaO was added to the ternary PbO-B_2O_3-TiO_2 system. The range of the BaO content for glass-forming was 7.5 mol%–20 mol% in the 30PbO-(40-x) B_2O_3-30TiO_2-xBaO glass compositions. In this system, the eutectic effect was observed at the composition containing 12.5 mol% BaO, which readily produced a stable glass from the melt by natural cooling. The glass-forming ability increased as the temperature ratios of T_c/T_l or T_g/T_l increased and as the temperature ratio of T_g/T_c decreased. Using the Vogel-Fulcher relation, the correlation between these temperature ratios was made by a plot of $1/(T_r\text{-}T_{rg})$ versus T_r and by considering the minimal temperature interval of cooling for bypassing the crystallization temperature zone. This confirmed that the glass formation tendency can be explained in terms of the ratios of transition temperatures of glasses, which may offer a useful tool to estimate glass-forming ability.

Acknowledgment

This work was supported by the KOSEF through the CPRC at Hanyang University.

References

1. M. H. LEWIS, in “Glasses and Glass-Ceramics” (Chapman & Hall, London-New York, 1989).
2. G. W. McLELLAN and E. B. SHAND, in “Electronic Components in Glass Engineering Handbook” 3rd ed. (McGraw-Hill Book Co., 1984).
3. P. F. JAMES, *J. Non-Cryst. Solids* **181** (1995) 1.
4. F. W. MARTIN, *Phys. Chem. Glasses* **6**(4) (1965) 143.
5. C. G. BERGERON and C. K. RMSELL, *J. Amer. Ceram. Soc.* **48**(3) (1965) 115.
6. D. G. GROSSMAN and I. O. ISARD, *ibid.* **52**(4) (1969) 230.
7. M. TAKASHIGE and T. NAKAMURA *et. al.*, *Japanese J. Appl. Phys.* **19**(5) (1980) L255.
8. K. KUSUMOTO and T. SEKIYA, *Mat. Res. Bull.* **28** (1993) 885.
9. M. J. REECE, C. A. WORRELL, G. J. HILL and R. MORRELL, *J. Amer. Ceram. Soc.* **79**(1) (1996) 17.
10. J.-J. SHYU and Y.-S. YANG, *ibid.* **78**(6) (1998) 1463.
11. S. R. ELLIOTT, in “Physics of Amorphous Materials” (Longman, London-New York, 1984) p. 13.
12. L. D. PYE, H. J. STEVENS and W. C. LACOURSE, in “Introduction to Glass Science: The Vitreous State” (Plenum Press, New York, 1972) p. 1.
13. H. RAWSON, in Proceedings of the IV International Congress on Glass, Paris (1956) p. 62.
14. M. COHEN and D. TUMBULL, *Nature* **189** (1961) 131.
15. Z. STRNAD, in “Glass-Ceramics Materials” (Elsevier, Amsterdam, 1986) p. 19.

Received 18 April 2001
and accepted 16 January 2002